JOURNAL OF OPTOELECTRONICS AND ADVANCED MATERIALS Vol. 18, Iss. 1-2, January – February 2016, p. 34-38

Influence of heat treatment and illumination on the vibration modes of $(As_4S_3Se_3)_{1-x}Sn_x$ thin films

O. V. IASENIUC[a], M. ENACHESCU[b], D. DINESCU[b], M. S. IOVU[a], S. A. SERGHEEV[a]
[a]Institute of Applied Physics, Str. Academiei 5, MD-2028 Chisinau, R. Moldova
[b]Centre for Science and Nanotechnology, Splaiul Independentei 313, Bucharest, Romania

Optical investigation such as infrared (IR) absorption and Raman spectra are efficient methods for obtaining information on the local structure of the disordered material, especially when the composition is varied. In this paper are reported the optical absorption and Raman spectra of chalcogenide glasses $(As_4S_3Se_3)_{1-x}Sn_x$ (x=0÷0.1) and amorphous thin films as-deposited, illuminated and heat treated. For ternary $As_4S_3Se_3$ chalcogenide glasses the absorption bands of S-H (Se-H) and H_2O located at ν=5190 cm^{-1} and ν=3617 cm^{-1}, characteristic for vitreous As_2S_3 are essentially reduced respectively. The Raman spectra of chalcogenide glasses and thermally deposited amorphous $(As_4S_3Se_3)_{1-x}Sn_x$ thin films consist of two broad bands located at around ν=236 cm^{-1} and ν=345 cm^{-1}, which corresponds to the symmetric stretching vibration modes of $AsSe_{3/2}$ and $AsS_{3/2}$ pyramids, respectively. Tin impurities didn't change the shape of Raman spectra, but shift the both bands to low frequency region. The light exposure of amorphous $(As_4S_3Se_3)_{1-x}Sn_x$ thin films shifts the main maximums of Raman spectra toward the lower frequencies region and decreases the picks intensities.

(Received November 02, 2015; accepted February 10, 2016)

Keywords: Chalcogenide glasses, Amorphous films, Raman spectra, Vibration modes

1. Introduction

Ghalcogenide glassy As_2S_3, As_2Se_3 are promising candidates for optoelectronic applications due to high chemical stability, high transmission in the IR region, high refractive index and non-linearities, low phonon energy, aand photoinduced effects. [1-4]. Optical investigation such as IR absorption, reflectance and Raman spectra are efficient tools for obtaining information on the local structure of the disordered material, especially when the composition is varied [5-7]. It was demonstrated that doping of chalcogenide glasses with metal impurities shift the main bands of Raman spectra to the low frequency region and lead to the appearance of the additional vibration bands in the low frequency spectral range. In addition, the Raman spectra was successfully used for investigation the photoinduced transformation and structural changes after the heat treatment and illumination in amorphous As-based thin films [8,9]. Some experimental results on the IR spectra and Raman spectra of bulk $(As_4S_3Se_3)_{1-x}Sn_x$ glasses are reported in [1,10]. In the present paper we report experimental results on IR, UV-VIS absorption, and Raman spectra of $(As_4S_3Se_3)_{1-x}Sn_x$ chalcogenide glasses and amorphous thin films as-deposited, light exposed and heat treated.

2. Experimental

The bulk $(As_4S_3Se_3)_{1-x}Sn_x$ (x=0÷0.1) chalcogenide glasses were prepared from the elements of 6N (As, S, Se, Sn) purity by conventional melt quenching method. The starting components $As_4S_3Se_3$ and Sn were mixed in quartz ampoules and then evacuated to pressure of $P\sim10^{-5}$ torr, sealed and heated to temperature T=900 °C at the rate of 1 °C/min. The quartz tubes were held at this temperature for 48 hours for the homogenization and then slowly quenched in the furnace. The thin film samples of thickness d=0.5÷3.0 μm were prepared by flash thermal evaporation in vacuum of the synthesized initial glasses onto glass substrates held at T_{subs}=100 °C. For optical transmission spectra measurements a UV/VIS (λ=300÷800 nm), the 61 NIR (λ=800÷3500 nm) Specord's CARLZEISS Jena production and PerkinElmer Spectrum 100 were used.

For optical transmission spectra measurements a UV/VIS (λ=300÷800 nm), the 61 NIR (λ=800÷3500 nm) Specord's CARLZEISS Jena production and PerkinElmer Spectrum 100 were used. The Micro-Raman measurements was performed using a Horiba LabRam 800 with an CW excitation working at λ=633 nm (P=17 mW) and at λ=532.18 nm (P=50 mW), in the spectral range ν=100-2500 cm^{-1}. The 800 focal length spectrograph was equipped with two switcheable gratings in the spectral range λ=200 – 1600 nm. The spectral resolution in the UV region was ν=1.5 cm^{-1}, in the VIS region - ν=0.6 cm^{-1}, and in the NIR region ν=0.3 cm^{-1}.

3. Experimental results and discussion

3.1. Optical absorption spectra

IR absorption spectra for some $(As_4S_3Se_3)_{1-x}Sn_x$ bulk chalcogenide glasses are presented in Fig.1.

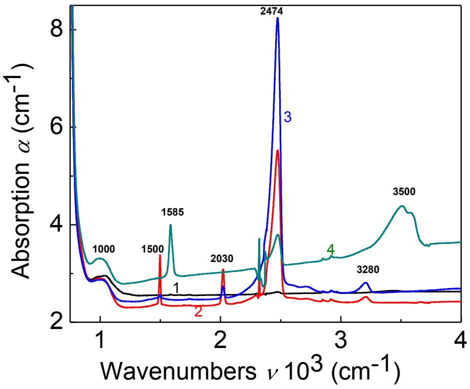

Fig.1. IR absorption spectra of bulk chalcogenide glasses $(As_4S_3Se_3)_{1-x}Sn_x$: x=0 (1), x=0.02 (2), x=0.06 (3), x=0.10 (4).

As as in the case of vitreous As_3S_3 doped with metals [9], the IR absorption spectra are characterized by several well resolved absorption bands.

For vitreous As_2S_3 these bands are located at the frequencies ν=5190 cm^{-1} (S-H), ν=3617 and 3522 cm^{-1} (H_2O), ν=2482 cm^{-1} (S-H), ν=1857 cm^{-1} (As-H), ν=1597 cm^{-1} (H_2O), and ν=1003 cm^{-1} (As_2O_3) [9]. The characteristic absorption bands for pure As_2S_3 are significantly reduced for the composition $As_4S_3Se_3$. For the $(As_4S_3Se_3)_{1-x}Sn_x$ glasses appear additional absorption bands located at ν=3280, 2030, and 1500 cm^{-1}. The observed changes upon doping in the mid IR region are most likely related to interactions of a portion of the introduced metal ion impurities with the inherent impurities of the host glass, such as hydrogen and oxygen atoms. Such interactions result in the reduction of the relative intensity of bands associated with O-H, S-H, As-O and As-H bonds in the parent glass [1].

Fig.2 represents the the absorption spectra of $(As_4S_3Se_3)_{1-x}Sn_x$ glasses and amorphous thin films in the Tauc co-ordinates $(\alpha \cdot h\nu)^{1/2}$ *vs.* $(h\nu)$.

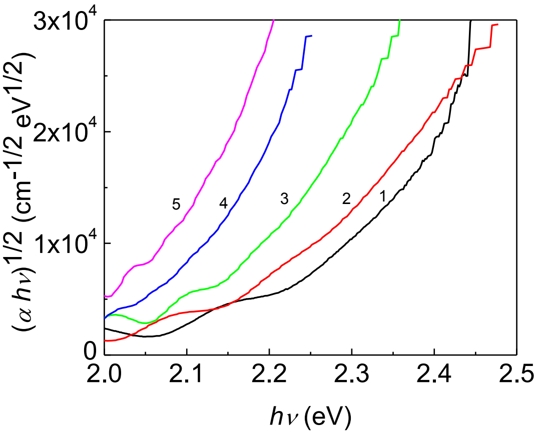

Fig.2. The dependence $(\alpha \cdot h\nu)^{1/2}$ vs. $(h\nu)$ of amorphous $(As_4S_3Se_3)_{1-x}Sn_x$ thin films: x=0 (1), x=0.01 (2), x=0.03 (3), x=0.05 (4), x=0.07 (5).

The absorption edge in the high absorption region (α>10^4 cm^{-1}) is described by a quadratic function

$$\alpha \propto \frac{1}{h\nu}(h\nu - E_g)^2, \qquad (1)$$

and when plotted in the Tauc co-ordinates $(\alpha \cdot h\nu)^{1/2}$ *vs.* $(h\nu)$ gives the value of the optical band gap E_g^{opt}, determined as the energy difference between the onsets of exponential tails of the allowed conduction bands. For amorphous $(As_4S_3Se_3)_{1-x}Sn_x$ thin films we obtain the values of optical band gap E_g^{opt}= 2.17 eV for x=0, and E_g^{opt}= 1.98 eV for x=1.0. For amorphous As_2S_3 the value of band gap was found to be E_g^{opt}=2.34 eV [11].

In the Urbach edge region ($\alpha \approx 1 \div 10^3$ cm^{-1}) the absorption coefficient spectra depend exponentially on the photon energy

$$\alpha \propto \exp\left(\frac{h\nu}{\Delta_l}\right), \qquad (2)$$

where Δ_l is the parameter which characterises the distribution of localised states in the band gap. The parameter Δ_l increase with the Sn concentration in the $(As_4S_3Se_3)_{1-x}Sn_x$ glasses from Δ_l=0.012 eV for x=0 upon Δ_l=0.072 eV for x=0.10, as in the case of $AsSeSn_x$ [6] and As_2S_3 doped with rare earth ions [9]. The broadening of the Urbach tail is caused probably by the formation of new impurity metal-based structural units, which add compositional disorder to the existing structural disorder.

3.2. Raman spectra

Raman spectra of bulk As_2S_3, As_2Se_3, and $(As_4S_3Se_3)_{1-x}Sn_x$ chalcogenide glasses were reported in [1]. It was shown that the Raman spectra of $As_4S_3Se_3$ glasses consist of two broad bands located at around ν=236 cm^{-1} and ν=341 cm^{-1}, which correspond to the main vibration modes of vitreous As_2Se_3 and As_2S_3, and are attributed to the symmetric stretching vibration modes of $AsSe_{3/2}$ and $AsS_{3/2}$ pyramids, respectively. It was shown that tin impurities in $(As_4S_3Se_3)_{1-x}Sn_x$ glasses decrises the intensity of the peaks located around ν=236 cm^{-1} and ν=341 cm^{-1}, and shift it towards the low frequency region of the spectra.

Raman spectra of as-deposited amorphous $(As_4S_3Se_3)_{1-x}Sn_x$ thin films are similar to those of bulk glasses and have the same features [1]. Doping of amorphous $(As_4S_3Se_3)_{1-x}Sn_x$ thin films with Sn impurities also shift the vibration bands situated at ν=236 cm^{-1} and ν=341 cm^{-1} in the low frequency region of the spectra.

The Raman spectra of amorphous $(As_4S_3Se_3)_{1-x}Sn_x$ thin films also were measured after the heat treatment at temperature T_{treat}=210 °C during t=30 min and after light exposure. Fig.3 represents the Raman spectra of some amorphous $(As_4S_3Se_3)_{1-x}Sn_x$ thin films for x=0 (curve 1), x=0.04 (curve 2), x=0.07 (curve 3), heat treated at temperature T_{treat}=210 °C during t=30 min. The heat treatment decrease the intensity of the vibrations peaks located at ν=236 cm^{-1} and ν=341 cm^{-1}, and sifts it in the low frequency region of the spectrum.

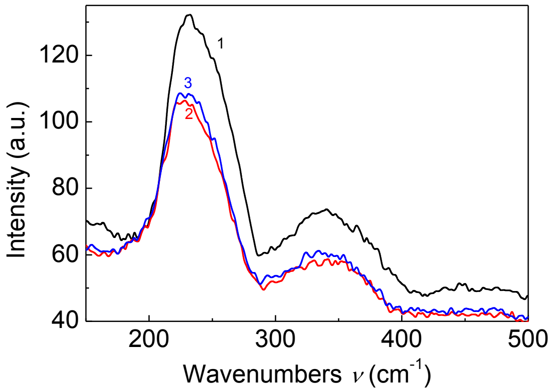

Fig. 3. Raman spectra of amorphous $(As_4S_3Se_3)_{1-x}Sn_x$ *thin films for x=0 (curve 1), x=0.04 (curve 2), x=0.07 (curve 3), heat treated at temperature* T_{treat}*=210 °C durin t=30 min.*

Fig.4 shows the Raman spectra of three compositions of amorphous films after the light exposure. Illumination of the amorphous $(As_4S_3Se_3)_{1-x}Sn_x$ thin films was perfomed with high intensity of the He-Ne laser (λ=532.18 nm and P=1 mW), which created a dark spot on the film due to the photostructural transformations (so call photodarkening, Fig.5). All measurments of the Raman spectra were perphormed at low intensity of the laser beam (P=0.02 mW), wich does not initiated the photodarkening effect. It is well known that the photoinduced effect in amorphous $(As_4S_3Se_3)_{1-x}Sn_x$ thin films is very pronounced [12].

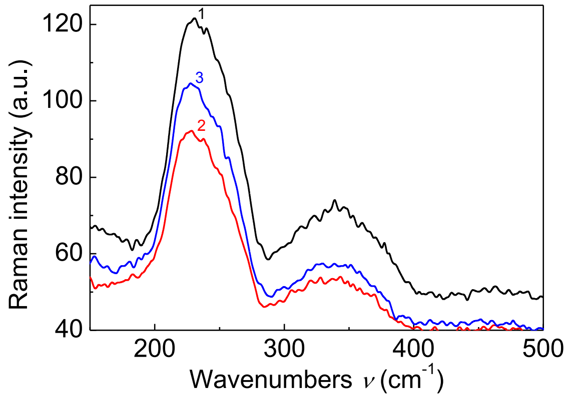

Fig. 4. Raman spectra of illuminated with He-Ne laser (λ*=532.18 nm and P=1 mW) of amorphous* $(As_4S_3Se_3)_{1-x}Sn_x$ *thin films: x=0 (curve 1), x=0.04 (curve 2), x=0.07 (curve 3).*

The light exposures decrease the intensity of the main vibration peaks, and slightly shift it in the high frequency region. As was pointed out in [13,14], the Raman spectra structure of evaporated amorphous thin films differs from the glass one and the molecular structure can be presented in the form of matrix, which consists of pyramidal units $AsS_{3/2}$, $AsSe_{3/2}$ and $AsS(Se)_{2/2}$. This matrix also can contain considerable amount of $As_4S(Se)_4$ and $S(Se)_n$ fragments which contain As-S and S(Se)—S(Se) homopolar bonds. Beside that, in the structure of the amorphous $(As_4S_3Se_3)_{1-x}Sn_x$ thin films can be presented and other structural units like tetrahedral $Sn(Se_{1/2})_4$, quasi-octahedral SnSe, and clusters such as of $SnSe_2$, as was demonstrated for the amorphous As_2Se_3:Sn_x thin films from the X-Ray Diffraction, Modulated Differential Scanning Calorimetry (MDSC) and Mössbauer spectroscopy measurements [7,15]. From the presented Raman spectra of the amorphous $(As_4S_3Se_3)_{1-x}Sn_x$ thin films we can assume that the annealing and light exposure has no influence on the structure of the material, as was demonstrated for the amorphous $Ge_xAs_ySe_{100-x-y}$ thin films [16].

Fig. 5. Pattern of the dark spot after light exposure of amorphous $(As_4S_3Se_3)_{0.93}Sn_{0.07}$ *thin films with beam laser (*λ*=532.18 nm, P=1 mW).*

Peak analysis using the deconvolution procedure for amorphous $(As_4S_3Se_3)_{1-x}Sn_x$ thin films show some features at the frequencies ν=186, 215.13, 225, 236, 251.37, 325.43, 345, 362.25, 436, 87, 473, 495, 47 cm^{-1} (Fig.6), and are similar for those of bulk glasses [17]. The presence of the structural units containing homopolar bonds in the structure of as-deposited amorphous As_2S_3, As_2Se_3 and $As_4S_3Se_3$ thin films can be explained by the thermal dissociation reaction during evaporation. Due to fast condensation of vapor on the cold glass substrate, these structural units are frozen in the structure of as-deposited amorphous films, and they are responsible for the fotosensibility and for the photodarkening processes of these films [18]. The concentration of the homopolar bonds, which is higher in the structure of as-deposited amorphous films, is reduced by exposure to light, and the structure of the amorphous thin film becomes closer to the structure of the bulk glass, as was demonstrated in for amorphous $As_{40}S_{60-x}Se_x$ thin films. This polymerization process seems to be reversed by thermal annealing, as was demonstrated for amorphous As_2S_3 [9,19]. From Raman spectroscopy of glasses $As_{40}S_xSe_{60-x}$ were determined and calculated by Gaussian software based on Density functional theory the frequencies of AsS_nSe_{3-n} clusters [20]. According to this work, the vibrational frequencies around ν=225, 251, 325, 362 cm^{-1} can be attributed to the clusters of molecular type $AsSe_3$, $AsSSe_2$, AsS_2Se and AsS_3, respectively.

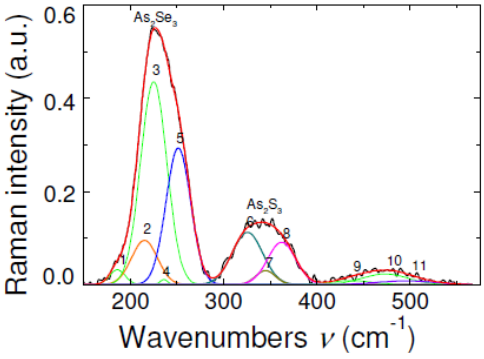

Fig.6. Deconvolution of the Raman spectra for light exposed amorphous $(As_4S_3Se_3)_{0.93}Sn_{0.07}$ thin films.

Recently it was shown that the amorpfous chalcogenide films As_2S_3 and $(As_4S_3Se_3)_{1-x}Sn_x$ are sensitive to the e-beam exposure also [21, 22]. These photoinduced effects which results in photostructural- and electron beam transformation, a increasing of the refractive index, allow creating in the amorphous chalcogenide films different diffractive relief structures with high resolution by holographic methods and by direct e-beam writing. As an example Fig.7 shows the AFM image modulation of the surface relief of the diffractive grating formed by e-beam writing in amorphous $As_4S_3Se_3$-Sn thin film.

The experimental results show that increasing of the e-beam current leads to increasing of the depth of the relief in amorphous film. We can conclude that the sharp increasing and high value of the diffraction efficiency are attributed to modulation process of the amorphous film surface, induced by e-beam irradiation. It is well known that the darkening portion of the grating (illuminated) interact with light in the higher degree, that the lightening one (not illuminated), because the photo-structural changes (the modulation of the optical constants) in the first regions take place more intensively, due to more strong absorption of the incident photons with the respective energy, and as a consequence of the shift of the absorption edge in the red region of the spectrum.

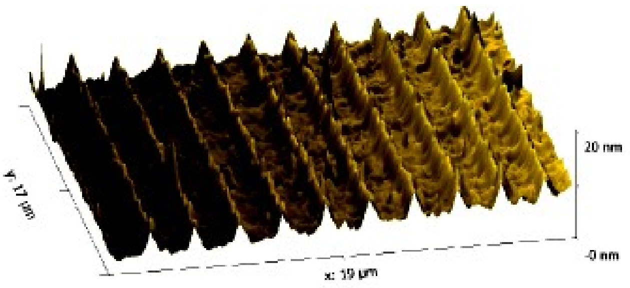

Fig.7. The modulation of the surface relief of the amorphous As4S3Se3-Sn thin films after the e-beam exposure.

In the light regions the velocity of the photo-structural changes smaller due to low sensitivity to the radiation. Electron irradiation results to some increasing of absorption of He-Ne laser irradiation. Due to this the absorption of readout laser beam in the range of grating is modulated by e-beam recording. Therefore the increasing of efficiency of gratings can be attributed to increasing of depth of refraction index modulation, caused by non-uniform light absorption which is evidently stronger in the e-beam irradiated areas of recorded gratings than in non-irradiated ones.

4. Summary

For ternary $As_4S_3Se_3$ chalcogenide glasses the absorption bands of S-H (Se-H) and H_2O located at ν = 5190 cm^{-1} and ν = 3617 cm^{-1}, characteristic for vitreous As_2S_3 are essentially reduced respectively. For amorphous $(As_4S_3Se_3)_{1-x}Sn_x$ thin films the optical band gap decrease from E_g^{opt}= 2.17 eV for x=0 up to E_g^{opt}= 1.98 eV for x=1.0. Raman spectroscopy was used for characterization of amorphous $(As_4S_3Se_3)_{1-x}Sn_x$ thin films. It was shown that Sn impurity influences the Raman spectra and shifts the main vibration bands in the low frequency region. The maximums situated at around ν=236 cm^{-1} and ν=345 cm^{-1} in the Raman spectra are characteristic for all investigated amorphous $(As_4S_3Se_3)_{1-x}Sn_x$ thin films and are attributed to the symmetric stretching vibration modes of $AsSe_{3/2}$ and $AsS_{3/2}$ pyramids, respectively. The light exposure and heat treatment of amorphous $(As_4S_3Se_3)_{1-x}Sn_x$ thin films also shift the main maximums of Raman spectra in the low frequency region. The obtained experimental results are discussed in framework of the molecular structure model of chalcogenide glasses suggesting of new tethraedral structural units like $SnSe_2$. It was shown that the observed photoinduced effects in amorphous films under light exposure can be used for formation of diffractive structures with high resolution.

Acknowledgement

This work was supported by the project no. 15.817.02.03A of the SCSTD of the ASM, project ASM-ANCS no. 13.820.05.15/RoF, as by the Romanian Executive Agency for Higher Education, Research, Development and Innovation Funding (UEFISCDI) through the program PN-II "Capacitati" under contract No. 686/22.04.2013.

References

[1] O. Iaseniuc, M. Iovu, M. Badea, I. Boerasu, M. Enachescu, Proc. of SPIE 9258, 92580N (2014).
[2] H. Jain, M. Vlcek, J. Non-Cryst. Solids **354**, 1401(2005).
[3] S.R. Zakery Elliott, J. Non-Cryst. Solids **330**, 1 (2003).
[4] I. Blonskyi, V. Kadan, O. Shpotyuk, M. Iovu, I. Pavlov, Optical Materials, **32**, 1553 (2010).
[5] E. I. Kamitsos, J. A. Kapoutsis, I.P. Culeac, M.S. Iovu, J. Phys. Chem., **B 101**, 11061 (1997).
[6] M. Iovu, S. Shutov, J. Optoelectron. Adv. M. **1**(1), 27 (1999).

[7] M. S. Iovu, E.I. Kamitsos, C.P.E. Varsamis, P. \ Boolchand, M. Popescu, J. Optoelectron. Adv. M. **7**(3), 1217 (2005).

[8] A. V. Stronski, M. Vlcek, A. I. Stetsun, A. Sklenar, P. E. Shepeliavyi, J. Non-Cryst. Solids **270**, 129 (2000).

[9] M. S. Iovu, S. D. Shutov, A. M. Andriesh, E.I. Kamitsos, C. P. E. Varsamis, D. Furniss, A. B. Seddon, M. Popescu, J. Optoelectron. Adv. M. **3**(2), 443 (2001).

[10] O. V. Iaseniuc, Moldavian Journal of the Physical Sciences, **11(**1-2), 58-(2012).

[11] M. Popescu, A. Andriesh, V. Chiumach, M. Iovu, S. Shutov, D.Tsiuleanu. The Physics of Chalcogenide Glasses, Ed. Stiintifica Bucharest - I.E.P.Stiinta, Chisinau, 1996**.**

[13] O. V. Iaseniuc, M.S. Iovu, I.A. Cojocaru, Moldavian Journal of the Physical Sciences, **13**(1-2), 44 (2014).

[14] A. V. Stronski, M. Vlcek, P. F. Oleksenko, Semiconductor Physics, Quantum Electronics & Optoelectronics **4**(3), 210 (2001).

[15] A. V. Stronski, M. Vlcek, S. A. Kostyukevych, V. M. Tomchuk, E. V. Kostyukevich, S. V. Svechnikov, A. A. Kudryavtsev, N. L. Moskalenko, A. A. Koptyukh, Semiconductor Physics, Quantum Electronics & Optoelectronics **5**(3), 284 (2002).

[16] M. S. Iovu, P. Boolchand, D. G. Georgiev, S. M. Iovu, M. Popescu, V. Ciorba, E. P. Colomeico, Moldavian \ Journal of the Physical Sciences **3**(3-4), 272 (2004).

[17] P. Nemec, S. Zhang, V. Nazabal, K. Fedus, G. Boudebs, A. Moreac, M. Cathelinaud, X.-H. Zhang, Optics Express, **18**(22), 22944 (2010).

[19] O. V. Iaseniuc, M. S. Iovu, G. F. Volodina, M. Enachescu, D. Dinescu, J. Optoelectron. Adv. M. **17**(7-8), 980 (2015).

[20] M. Vlcek, J. Prokop, M. Frumar, Int. J. Electr. **77**(6), 969 (1994).

[21] P. Hari, T. Su, P.C. Taylor, P.L. Kuhns, W.G. Moulton, N.S. Sullivan, J. of Non-Crystalline Solids **266&269**, 929 (2000).

[22] X. Han, H. Tao, L. Gong, J. Han, S. Su, Chalcogenide Letters, **11**(4), 181 **(**2014).

[23] S. A. Sergheev, M. S. Iovu, Journal of Nanoelectronics and Optoelectronics **7**, 740 (2012).

[24] S. A. Sergheev, M. S. Iovu, O. V. Iaseniuc, Proc. of SPIE, **9258**, 92580S-1 (2015).

---

*Corresponding author: oxana.iaseniuc@phys.asm.md